Electrical Power and Energy Systems 169 (2025) 110773

Contents lists available at ScienceDirect

International Journal of Electrical Power and Energy Systems

journal homepage: www.elsevier.com/locate/ijepes

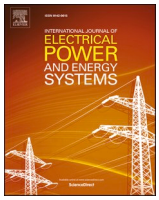

Contribution analysis of neutral current for the substations invaded by stray current from multiple metro lines

Ye Cao [a], Song Xiao [a,*], Jingdong Yan [a], Chenyang Liu [a], Tiangeng Li [a], Xiao Liu [a], Guangning Wu [a], Yujun Guo [a], Jiefu Hou [a], Yongdong He [a], Xueqin Zhang [a], Nibishaka Erneste [a], Jan K. Sykulski [b]

[a] School of Electrical Engineering, Southwest Jiaotong University, Chengdu, China
[b] University of Southampton, Southampton, England, United Kingdom

ARTICLE INFO

Keywords:
Stray current
Neutral current
Frequency domain analysis
Contribution degree calculation

ABSTRACT

As a type of convenient and environmentally friendly transportation tool, urban rail transit has been constructed as vital infrastructure in numerous cities over the world. Currently, direct current (DC) traction power supply mode has been applied as mainstream for most of metro lines. However, along with long-term service, the insulation performance between steel track and concrete sleeper deteriorates gradually, possibly causing traction current leaking from rail to ground, forming as 'stray current'. It possibly invades into transformers through their grounding poles, causing local thermal surge, abnormal vibration or even power quality degradation. At present, only relying on the passively protecting method via installing fixed impedance at the grounding pole can hardly cope with the transiently-varying stray current. Tracing the origin of stray current especially under the scenario of multiple metro lines becomes essential, as the periodicity of traction current from each metro line can be extracted as 'fingerprint'. A boundary element model of a region with multiple metro lines is launched based on practical geological data, for evaluating the route and distribution of stray current. Based on the Wavelet Transform (WT) method, the correlation is found precisely via comparing periodic feature between the traction current of different metro lines and the neutral current measured synchronously at substations. Moreover, an origin tracing method for clarifying the contributions made by different metro lines on the substation's neutral current is proposed via analyzing the local periodicity of traction current and neutral current, for laying the solid foundation of precise suppression from origin.

1. Introduction

For reducing carbon emission, the construction of novel infrastructures such as charging stations for electric vehicles (EVs), energy storage facilities and urban rail transit systems are crucial for promoting the expansion of renewable energy power in cities [1,2]. However, the leakage of the direct current (DC) from these infrastructures may directly bring a negative impact on the alternate current (AC) main grid [3]. Among the infrastructures in large cities, the metro is a highly effective solution for addressing transportation challenges in metropolitan cities. By the end of 2023, metro systems have been implemented in 157 cities worldwide, with a total length exceeding 41,000 km. Core cities like London, New York, Tokyo, and Beijing are notable examples, with complex metro networks covering over 70 % of their urban areas [4]. In practice, the degradation of the insulating performance between the rail and the ground may appear along with the long-term operation of metro lines [5]. Additionally, the accumulation of carbon dust generated by the sliding electrical contact between the pantograph strip and the catenary can create new conductive paths between the rail and the ground in closed metro tunnels [6]. Due to these factors, the 750 V/1500 V DC traction reflux might leak from the rail into the ground, forming the so-called 'Stray Current', which varies transiently along with the traction conditions of metro vehicles. More noteworthy, Stray current may also result in alternating neutral current in surrounding transformers, leading to the DC bias phenomenon, which can directly cause a local thermal surge of the transformer's iron yoke and the drastic vibration of windings [7,8], as shown in Fig. 1. The long-term vibration may significantly shorten the lifespan of transformers. Furthermore,

* Corresponding author at: Southwest Jiaotong University, Chengdu 611756, China.
E-mail address: xiaosong@home.swjtu.edu.cn (S. Xiao).

https://doi.org/10.1016/j.ijepes.2025.110773
Received 14 February 2025; Received in revised form 25 April 2025; Accepted 17 May 2025
Available online 19 May 2025

along with the total harmonic distortion of the current in over-saturated transformers increasing, a low power coefficient may result in loss increased, efficiency decreased, and power quality degradation potentially [9]. Even some weak electrical devices like current mutual inductors tend to be affected by stray current, with their accuracy reduced due to magnetic core saturation, which can lead to malfunctions in protective devices and the instability of the surrounding power system [10].

Given the increasingly prominent issue of the DC bias phenomenon associated with metro development, some researches have been undertaken about the generation and distribution characteristics of stray current generated by metro, via analyzing the varying tendency of the current measured at the transformer's neutral point [11], as some suppression measures for mitigating the DC bias phenomenon have been proposed [12,13]. The DC bias current flowing into the transformer from its earthing networks can be suppressed to some extent, via installing DC suppressors (resistors, capacitors, etc.) at the transformer's earthing pole [14]. Nevertheless, only applying the DC suppressors with fixed impedances, it is difficult to satisfy different operational conditions of the transformer, as especially during the train shutdown at night the impedance in series at the earthing pole does hinder the discharge of overvoltage generated by the operation of vacuum circuit breaker or thunder. If installing the DC suppressors at multiple substations, the action parameters of the global rely protection system have to be adjusted.

In urban areas, metro lines often intersect, making it common for multiple lines around a single substation. In such cases, the reason for causing vibration and noise in transformers might be the combined action of multiple lines. As it is extremely difficult to trace the source of the stray current, choking the stray current from the origin almost seems like an impossible mission. Only depending on applying the passive defense strategy at the affected substation, it is impossible to solve the DC-biased issue, besides the stray current varies dynamically due to the specific physical displacement and operational condition of metro vehicles [15]. It is challenging to assess the contribution of each metro line and develop corresponding mitigation measures for restraining stray current. In summary, analyzing the frequency domain characteristics of neutral current to determine the contribution of each metro line is a key approach to addressing the cumulative impact of multiple metro lines.

Currently, Fourier analysis has been employed to investigate pipeline potential fluctuations induced by stray current generated by metro, for identifying dominant frequency components in neutral current measured at the interfered substations [16]. The correlations between frequency-domain parameters of potentials and corrosion rates in metallic pipelines has been explored based on the subsequent studies [17]. However, it remains challenging to dig out the direct correlation between the frequency-domain characteristics of neutral current derived from Fourier analysis and the operational parameters of metro traction power system, primarily due to Fourier transform's inherent limitations in time–frequency analysis. In contrast, wavelet transform is particularly suitable for analyzing non-stationary time signal in highly time-varying metro traction systems. Similar to the periodic operation of metro systems, atmospheric and crustal changes also exhibit periodicity. Therefore, wavelet transform, commonly used in rainfall and earthquake analysis, was applied to analyze the potential fluctuation of metal pipelines caused by stray current in a few works [18]. The relationship between a single metro line and pipeline-ground potential fluctuation periods is explored based on wavelet power spectrum results, as there is no further work to verify the feasibility of this idea. In summary, current research has conducted frequency-domain analysis on metro stray current [19] with the induced anomalous soil potential distribution. However, no studies have yet employed wavelet transform analysis for neutral current characterization, nor has the relationship between neutral current and metro operational cycles been paid attention to.

Herein, both the traction current of metro and the current flowing through the neutral point of the substation are captured simultaneously to explore the correlation between the neutral current and stray current, via comparing their periodicity. A corresponding boundary element model based on the geological environment of a large city is launched, also involving the topology of its metro lines and power grid. The measured neutral current data from various substations tends to be analyzed by the optimal wavelet basic function to determine the correlation between the fluctuation periods of neutral current and metro systems. Based on the analysis of periodic proportions, a method for evaluating the contributions from multiple metro lines in real time is proposed, as the leakage origin with ratio can be analyzed. Based on the assessment of the leakage degree, can assist the relevant departments in determining if it is necessary to take remedial measures to improve the insulation performance between the rail and the ground. This traceability method for tracking the origin of stray current provides an effective pathway to prevent the leakage of DC traction current from the origins.

The main contributions of this study can be summarized as follows:

1) In Section 2, networked hall sensors are deployed at multiple substations in a metropolitan area to acquire neutral current simultaneously. Synchronized traction current variations are monitored through the on-board traction current monitoring system. A boundary element model incorporating stratified soil characteristics is

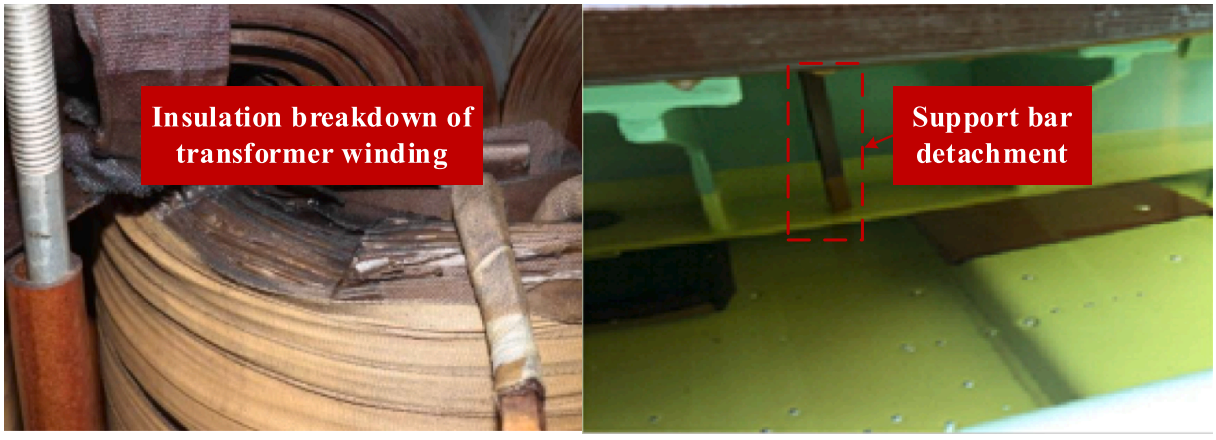

Fig. 1. The problem caused by stray current: (a) The insulation breakdown of transformer winding; (b) The detachment between support bar and transformer winding due to drastic vibration.

developed based on the geological survey data of the investigated region.

2) In Section 3, comparative analysis is conducted between Fourier transform and wavelet transforms employing different mother wavelets for frequency-domain analysis method of neutral current, as the wavelet transform methodology with Morlet wavelet basis is ultimately selected as the analytical tool, through systematic evaluation of time-synchronized datasets.
3) In Section 4, the correlation of travel duration within the section of adjacent stations and neutral current main fluctuation period is explored, as the distribution degree of two metro lines to neutral current is accessed, based on the difference of fluctuation periods proportion.

The rest of the paper is organized as follows: In Section 1, the adverse impacts of metro stray current on surrounding power system are briefly introduced. Previous works on mitigating stray current are also summarized, particularly highlighting the applications of Fourier transform and wavelet transform methodologies in related research domains. Conclusions are presented in Section 5.

2. The analysis of generating mechanism of stray current

2.1. The generating mechanism of stray current caused by the metro operation

2.1.1. The operational principle of the traction power supply system for metro

Before digging out the root causing stray current, it is necessary to understand the operational principle of the traction power supply system for metro. Initially, the terrestrial traction substation for supplying metro lines achieves the power from the 110 kV/220 kV three-phase AC power system. Then, the AC power tends to be converted into 750 V/1500 V DC power by rectifiers within the traction power substation (TPS). As the unique power entrance for the metro train, the pantograph-catenary system provides the power transmitting path via the sliding electrical contact between carbon strip and contact wire, as presented in Fig. 2.

2.1.2. The generating mechanism of stray current

In Fig. 3, the rail is fixed on both sides by fasteners and anchored on the ground, as an insulating mat embedded between the fasteners and concrete, along with sleeves installed on the spikes, are designed to maintain insulation between the rail and the ground. Apart from supporting the metro train, the rail as the main reflux channel also plays a vital role in sending the traction power back to the terrestrial substations. However, due to the long-term rolling contact between the wheel and the rail, the insulating property of the insulating mat might deteriorate, moreover, the carbon dust dropped from the sliding pantograph-catenary contact in the enclosed tunnels may accumulate on the surface of the rail. Based upon the interaction of these factors, the traction current might leak into the ground, as a part of the leakage current is unable to be captured by the drainage network, ultimately forming the so-called 'stray current'.

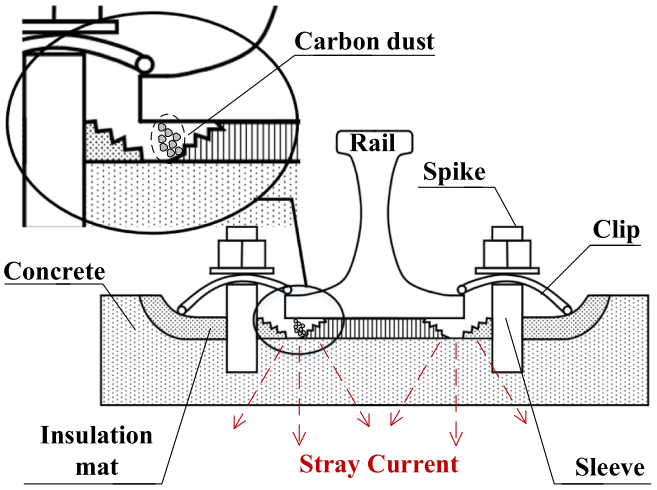

Fig. 3. The generation mechanism of stray current.

2.1.3. The acquisition method of both traction current of metros and neutral current of substations

The currently-existing research works can preliminarily judge DC-driven civic transportation as a prime suspect of generating stray current. However, lack of exploration of the features of both traction and neutral currents, it is extremely difficult to trace the origin of stray current, especially under the multi-metro lines scenario. Here, the specific acquisition methods for the traction current at the source end (metros) and the neutral current at the receiving ends (substations) are demonstrated as follows.

2.1.4. Source end — the acquisition method of the traction current of metros

Via analyzing the generation mechanism of stray current, it is found that the primary cause of stray current is the leakage of traction reflux in rails. In order to analyze the characteristics of stray current, it is essential to master the varying rules of traction current of the metro train. As shown in Fig. 4(a), there is a closed-loop hall effect sensor (Model CHV 5000B, ±0.5 % accuracy) installed on the train roof for measuring the high-voltage cable linking between the pantograph and the traction transformer. The traction current waveforms are pre-processed by anti-aliasing filters before being synchronously recorded by on-board traction current monitoring system, with time synchronization ensured by the vehicle-mounted timekeeping system, as the acquired data is transmitted to the data logging computer via the LAN interface using the TCP/IP wire with the data granularity from 200 to 1000 bytes per frame.

The varying tendency of traction current during a single operational cycle of the metro train, including starting, acceleration, uniform motion and slowdown, is presented in Fig. 5. The traction current varies regularly during a full operational cycle when the metro train runs between

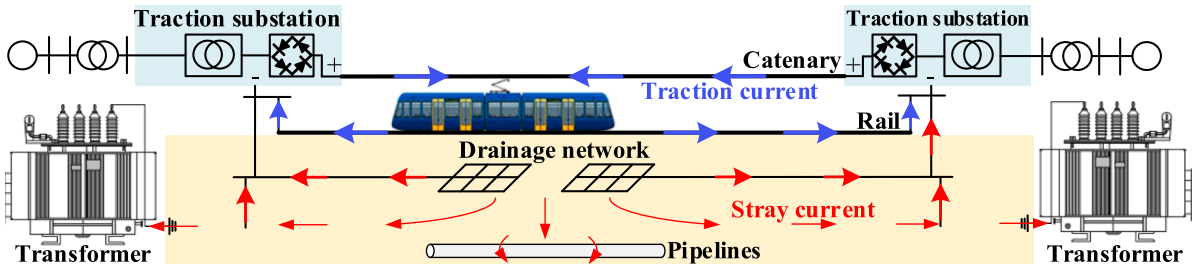

Fig. 2. The topology of traction power supply system.

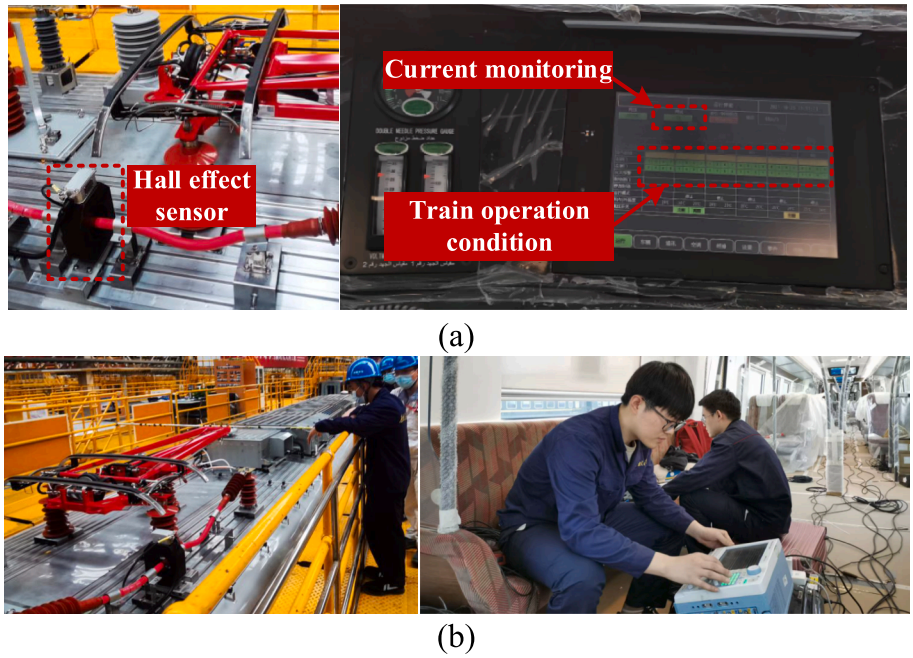

Fig. 4. The acquisition of traction current: (a) the installation of the vehicle-mounted Hall effect sensor with the metro controlling system; (b) the on-site photos.

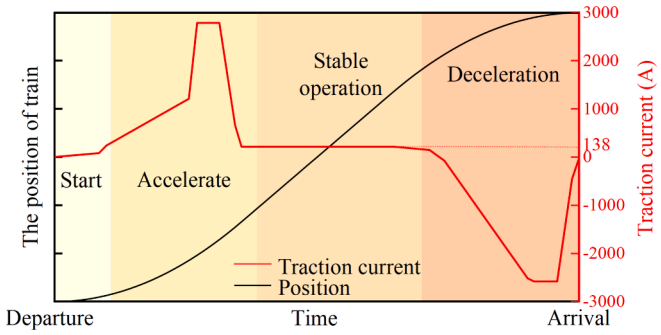

Fig. 5. The varying tendency of traction current during a single operational cycle of the metro train.

the adjacent stations, each of metro trains tends to experience several steps including starting, accelerating, uniformly operating and decelerating as shown in Fig. 5. Here, it is worth mentioning that the regenerative braking operation is triggered when the train decelerates, as the polarity of the traction current inverses, feeding back the terrestrial substation through the catenary. Thus, the amplitude of traction current alternates from positive and negative during an individual cycle of operation. Due to the Communication-Based Train Control (CBTC), the varying tendency of the traction currents for different trains along the given route remains relatively consistent, which indicates that the stray current may also show periodic characteristics. Although various metro trains all experience the same operational cycle step by step, the travel duration within the section of adjacent stations for each metro line might be subtly different.

Considering the strong periodicity of different metro lines, whether a 'fingerprint' library of the traction currents for different metro lines can be built for tracing the origin of leakage current attracts our attention deeply. Without precisely tracing the leaking origin of stray current, the blind implementation of suppressing measures for restricting stray current may bring some positive impact to the protected substations. However, probably the stray current shifted from the protected substations to those ignored substations.

2.1.5. Receiving end — the acquisition method of the neutral current of substations

Five typical substations near metro lines are selected. For collecting the current flowing through the grounding pole of substations, the real-time current monitoring devices are installed at these five substations. The monitoring device incorporates an open-loop Hall effect sensor (Model CHK-80Y21SP3, ±1 % accuracy) mounted on the transformer grounding busbar via an insulating clamp plate, maintaining a minimum clearance of 30 mm from the transformer enclosure to mitigate electromagnetic interference. The instrumentation specifications for DC current measurement are detailed in Table 1. All current-measured devices are calibrated against a Keysight B2961A precision DC current analyzer prior to deployment. Collected current data with corresponding timestamps can be transmitted to the on-line servers via a fifth generation (5G) mobile network. Through the analysis of the data collected synchronously, the correlation between the source of leakage current and the influenced substations can be explored, as the current acquisition process with the specific setting of testing sites is presented in Fig. 6.

The waveform of the neutral current measured at a Substation during a whole day is achieved, as shown in Fig. 7(a). According to the relevant standards [20,21], the neutral current at a 220 kV transformer should not exceed 4A, as indicated by the horizontal red line in Fig. 7. The varying tendency of the neutral current within a whole day reveals a strong correlation existing between the neutral current and metro traction current.

The specific proof is demonstrated as the neutral current remaining roughly zero during the non-operational hours of metro lines (00:00 am–06:00 am) and frequently exceeding the threshold (4A) during the metro normal operation period (20:00–22:00). The maximum amplitude of the neutral current occurs during peak hours (17:30–19:30), even reaching up to 9.88 A, which is approximately 2.47 times of the threshold value. The zoom-in snapshot of the neutral current waveform

Table 1
The Parameter of Current Measurement Device.

Measurement object	Type	Accuracy	Sampling rate
Traction current	CHK-80Y21SP3	±1 %	10 Hz
Neutral current	CHV-5000B	±0.5 %	1 Hz

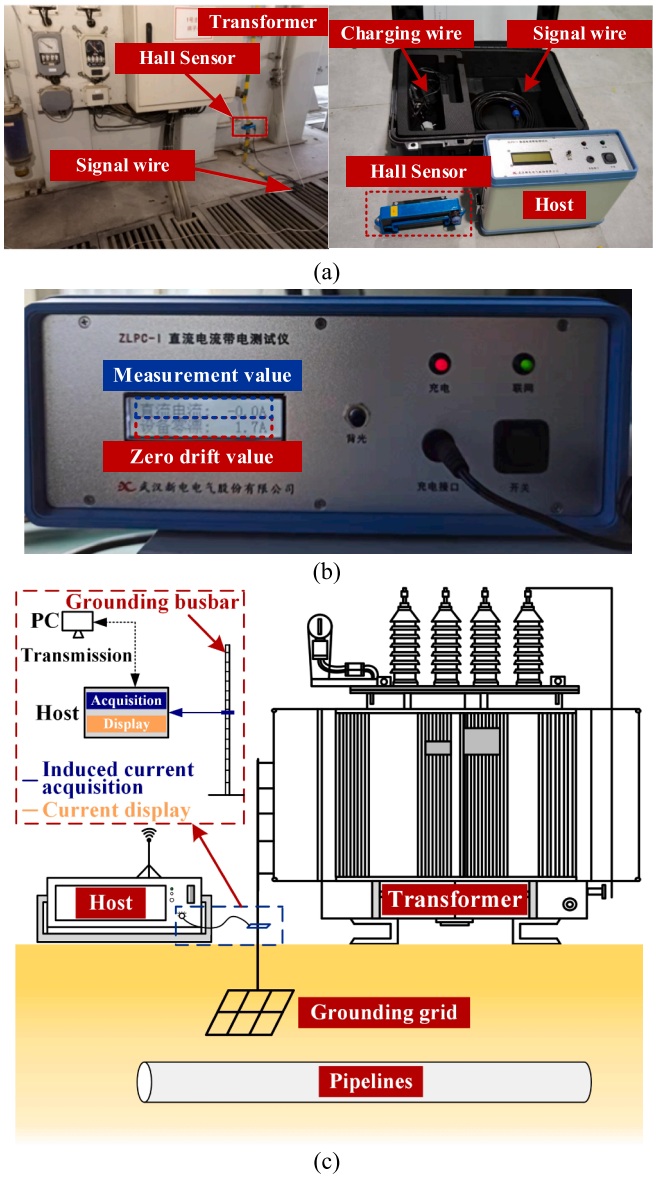

Fig. 6. The measurement of neutral current: (a) the photo of measurement equipment; (b) the automatic calibration procedures; (c) the measurement principle.

over 240 s (Fig. 7(b)) clearly shows that the neutral current does have similar periodicity and alternating characteristics with the traction current of the metro.

2.1.6. The construction of neutral current simulation model around multiple metro lines based on BEM

Considering the extensive region influenced by stray current, the boundary element method (BEM) as a highly efficient numerical tool can be employed to discretize the research object's boundary, for mitigating the computational complexity via reducing the dimensions and the number of processing nodes. Therefore, the neutral point current simulation model tends to be developed using SESCAD tool in the CDEGS software, with the critical initial setting presented in Table 2.

As the primary propagation path for stray current, the structure and resistance of soil directly determine the distribution of stray current. Via the geological investigation, the soil in the targeted region is alluvial plains, as the electrical parameters are listed in Table 3 and Fig. 8. The soil parameters were configured through the predefined horizontal multi-layer soil model in BEM software [22].

In Fig. 9, substations with 2 metro lines are contained in the stray current analysis model, as the connecting lines bridging between neighboring substations are also involved. At the metro stations, the catenary and rail for double rails along with the up and down directions are connected to describe the topology of the traction power supply system. Additionally, within the metro station, the stray current drainage network is connected to the structural steel bars.

The material parameters of the vital conducting components in the system including the traction substation, catenary, rail, current drainage network, and steel bars are detailed in Table 4. In the stray current analysis model, the metro train is designated as a mobile current excitation source. The train's entire operational process is discretized into 86,400 time-domain steps to simulate a full 24-hour cycle, with each step corresponding to a 1-second interval that serves as both the simulation timestep and the current sampling interval. A script is developed to automatically modify and generate new simulation models. In every model, the train's position in real time with corresponding traction current are dynamically adjusted according to its real-time operational state by this script.

Among the substations in the targeted region, Substation 2 is the closest to two metro lines, which tends to suffer the most serious impact of stray current. The varying tendency of the neutral current measured at the grounding pole of Substation 2 is achieved when the two metro lines operate simultaneously, as shown in Fig. 10. The deviation existing between simulating and experimental results are listed in Table 5. Via the comparison between simulating and experimental results, it can be found the deviation is maintained within 10 % averagely, which can be viewed as acceptable. Apart from time domain analysis, it is essential to analyze the characteristics of neutral current from the view of the frequency domain, which will be shown in Chapter IV.

The out-of-standard neutral current indicates that stray current generated by metro invades the transformer's winding through the grounding poles, which may bring a threat to the normal operation of substations. Via the preliminary analysis, there is a direct correlation existing between the variation of the neutral current and the operational cycle of metro lines. However, at this stage, the ingredient of the neutral current can hardly be analyzed only based on visual sightings. Thus, it is essential to apply some advanced algorithms to realize the features in the current data from both origins and substations.

3. The frequency domain analysis method of neutral current

Via establishing a fingerprint library including the stray currents generated from different metro lines, through comparing the fingerprint between traction current of metro lines and neutral current of substations the correlation existing between them is possibly explored. The commonly used methods include Fourier Transform (FT), Wavelet Transform, and Hilbert Transform (HT). The FT is currently the primary tool for analyzing neutral current. However, given the rapid short-term fluctuations of stray current and the need to analyze neutral current across different metro operational periods, this paper proposes using Wavelet Transform to analyze the fluctuation period of neutral current.

3.1. The specific introduction of FFT and wavelet transform

3.1.1. Fourier transform

As a fundamental technique of revealing the frequency components of a periodic signal, the Fourier Transform (FT) is able to convert signals from the time domain to the frequency domain, as at the initial stage the Discrete Fourier Transform (DFT) is selected to attempt the analysis of the neutral current waveform collected at the substations here. The expression of the DFT is defined as:

$$X(k) = \sum_{n=0}^{N-1} \sum x(n) W_N^{nk} \quad k = 0 \sim (N-1) \tag{1}$$

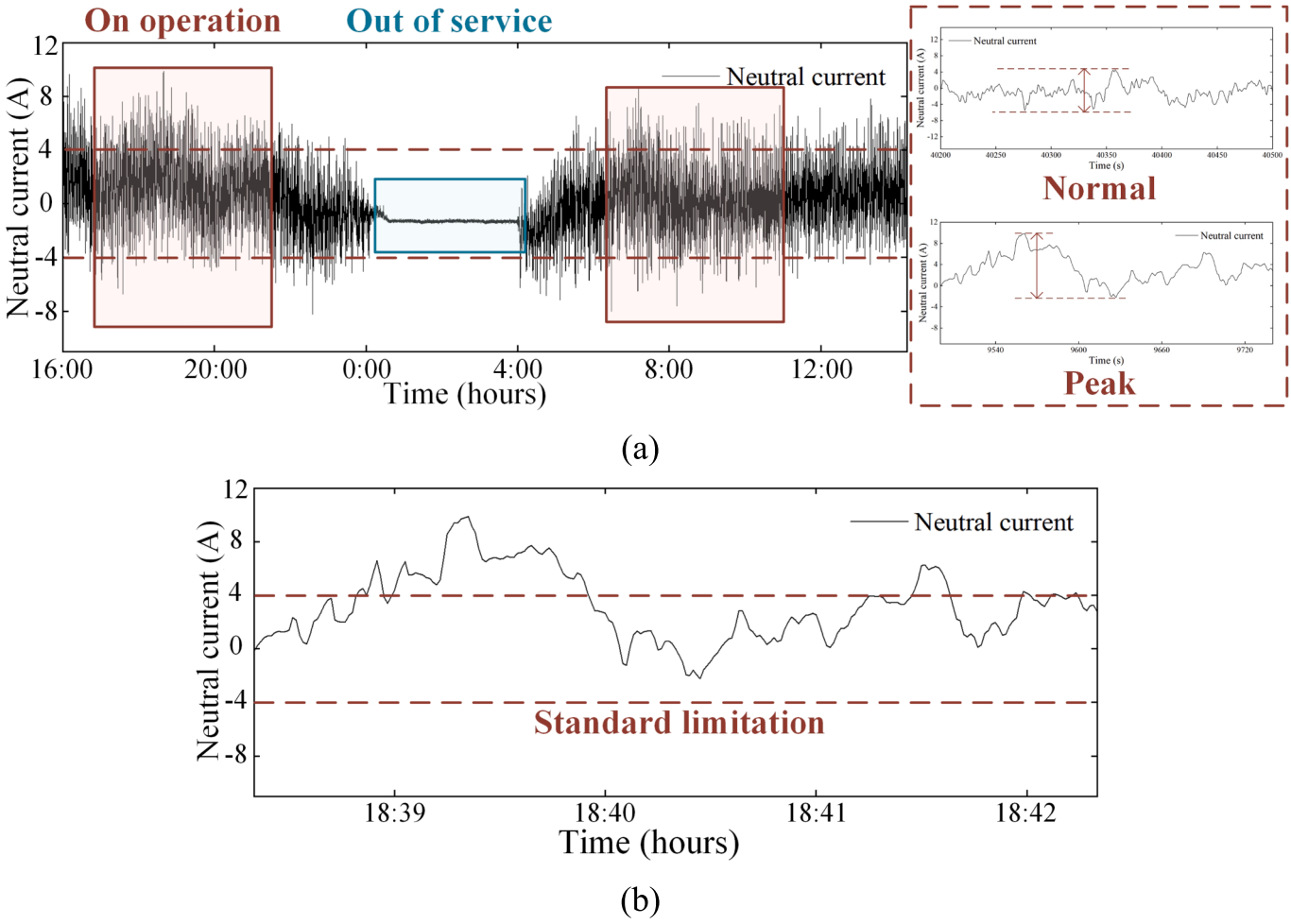

Fig. 7. Measured neutral current: (a) The neutral current waveform over one day; (b) The neutral current waveform over 200 s.

Table 2
The BEM Simulation Parameters.

Software version	Maximum iterations	Residual tolerance	Calculation setting	Calculation frequency
15.4.8190, Professional Edition	100 times	$<10^{-6}$	Scalar potential	Single-frequency

Table 3
The Layer Parameter of Soil.

Geological Layers	Soil layer	Resistivity (Ω·m)	Depth (m)
Top soil layer	Clayey soil(soft)	50	0–3.9
First sand layer	Chalky soil	180	3.9–8.4
First soft soil layers	Silty Clayey soil (soft)	20	8.4–10.3
Second soft soil layers	Clayey soil	60	10.3–16.6
Hard soil layers	Clayey soil (hard)	80	16.6–19.8
Second sand layers	Chalky soil	250	19.8–30

To enhance computational efficiency, the Fast Fourier Transform (FFT) algorithm is utilized here [23], the FFT reduces the number of operations by the symmetry, periodicity, and reducibility of the DFT's rotation factors W_N (Equation (2), significantly speeding up the computation without affecting the accuracy of the frequency domain analysis [24].

$$W_N^{nk} = e^{-j\frac{2\pi nk}{N}} \tag{2}$$

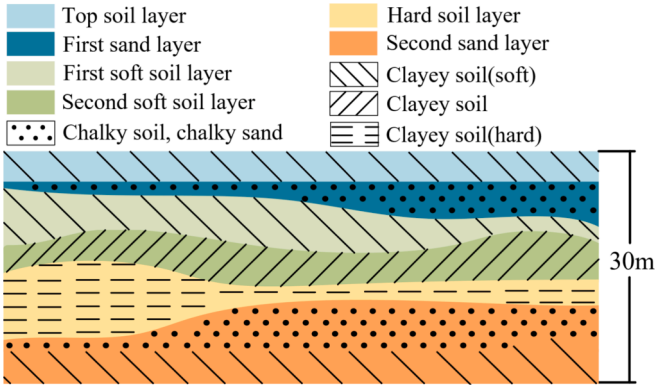

Fig. 8. The structure and parameter of soil.

where: N is the total number of samples, n and k are integer indices, j is the imaginary unit [25].

3.1.2. *Wavelet transform*

Wavelet Transform can be divided into Discrete Wavelet Transform (DWT) and Continuous Wavelet Transform (CWT). The DWT is primarily used for signal denoise and compression, while the CWT is suitable for frequency-domain analysis feature extraction from signals [26]. Therefore, this paper selects CWT as the frequency analysis method, with the expression as follows:

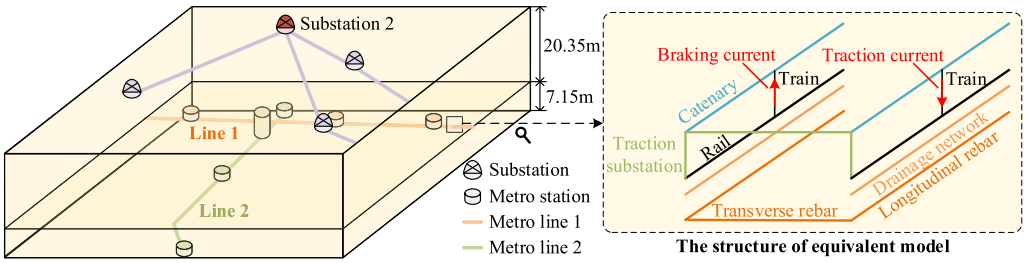

Fig. 9. The introduction of CDEGS model.

Table 4
The Material of Simulation Model.

Component	Unit length resistance (Ω/m)	Coating type	Boundary conditions
Traction substation	4.60×10^{-5}	Insulation	Dirichlet
Catenary	8.00×10^{-5}	Insulation	Dirichlet
Train	1.10×10^{-4}	Insulation	Dirichlet
Rail of Line 1	2.00×10^{-5}	To-ground resistance (2.08×10^{6}Ω/m)	Robin
Rail of Line 2	2.00×10^{-5}	To-ground resistance (3.15×10^{6}Ω/m)	Robin
Structure steel bar	8.00×10^{-6}	Default (0 Ω)	Neumann
Drainage network	2.00×10^{-5}	Default (0 Ω)	Neumann

$$W_{\mathrm{n}}^{X}(s) = \sqrt{\frac{\delta t}{s}} \sum_{\mathrm{n}'=1}^{N} x_{n'} \psi\left[(n'-n)\frac{\delta t}{s}\right] \tag{3}$$

Among this, the wavelet coefficient is represented as $W_{\mathrm{n}}{}^{X}(s)$; $\psi[]$ represents mother wavelet; δt is time step; s is the wavelet scale.

In addition to the frequency-domain analysis using wavelet coefficients, the cross-correlation function based on WT can explore the correlation between Signal x and Signal y. The peak of the cross-correlation coefficient $R_{xy}(k)$ indicates the degree of correlation between the two signals, with a higher value signifying a more significant influence of Signal x on Signal y. The coherence plot further reflects the phase relationship between the two signals.

$$R_{xy}(k) = \frac{C_{xy}(k)}{\sigma(x)\sigma(y)} \tag{4}$$

Among this, the covariance of Signal x and Signal y is represented by $C_{xy}(k)$, k is the delay time. $R_{xy}(k)$ is correlation number, $\sigma(x)$ and $\sigma(y)$ are the sample standard deviation of X_{n} and Y_{n} respectively.

3.2. The comparison of FFT results and wavelet transform results

To determine the most suitable frequency domain analysis method for neutral current, both FFT and wavelet transform methods are tried to extract the frequency-domain 'fingerprint' from the neutral current data recorded.

The frequency spectrum (0.00001 Hz–0.1 Hz) of the neutral current over a single day obtained through FFT is shown in Fig. 11(a). Although FFT can be utilized to analyze the frequency components of the current, for providing global information in the frequency domain. However, the FFT is more suited to periodic signals, as for the non-stationary signals like neutral current its performance of extracting features is not that satisfactory. The wavelet coefficients modulus map of Substation 1's neutral current over 30 min is presented in Fig. 11(b). The magnitude of wavelet coefficients can reveal the distribution of fluctuation periods within a specific time period. Unlike the FFT, wavelet transform allows for flexible analysis time settings, which are able to display periodic variation in different time intervals.

The variance of wavelet coefficients can indicate the fluctuation period of a signal, with the maximum variance corresponding to the primary fluctuation period. To verify which frequency domain analysis method is more suited for determining the fluctuation period of neutral current, we compared the FT period analysis results with the wavelet variance, as shown in Fig. 12. The results indicate that wavelet transform provides clearer indications of the fluctuation period.

Table 5
The Deviation Existing Between Simulating and Experimental Results.

Results source	Range of Fluctuation	Mean Absolute Error	Root Mean Square Error
Simulated results	−9.40–3.89	0.5163	0.6682
Experimental results	−9.79–3.98		

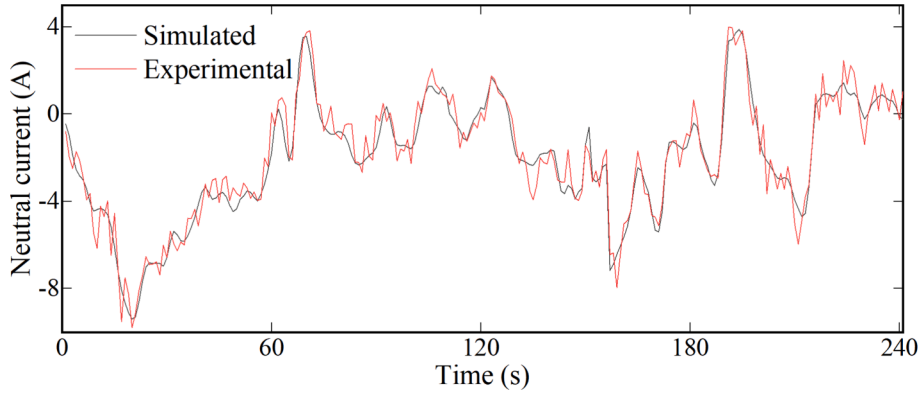

Fig. 10. The comparison of simulated neutral current and measured neutral current.

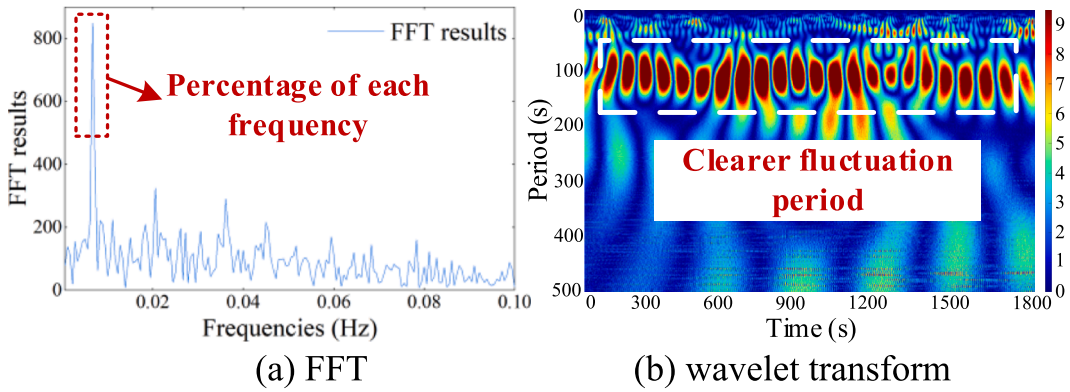

Fig. 11. The FFT and wavelet transform results.

The current sampling period for neutral current is a minimum of 1 s. While FFT has lower computational complexity than wavelet transform, a small amount of data over one day diminishes this advantage. Considering these factors, wavelet transform is ultimately chosen as the method for analyzing fluctuation periods.

3.3. *The selection of wavelet basis function*

The selection of an appropriate wavelet basis function is crucial for the wavelet transform analysis. Considering the non-stationary characteristics of stray current with its drastic variations over short term, the potential suitable wavelet basis functions for satisfying these features via investigation mainly contain Daubechies Wavelets, Biorthogonal Wavelets and Morlet Wavelets, which are worthy of trying. The comparison of the wavelet coefficient modules when applying these three different wavelet basis functions to analyze the neutral current captured from Substation 1 and Substation 2 over a single day is presented in Fig. 13. When applied to address the neutral current, the wavelet coefficient modules of Biorthogonal Wavelets across different periods show extremely limited variation, making it difficult to distinguish the primary fluctuation period (Fig. 13(a)). The wavelet transform results with Daubechies wavelets can basically represent the main fluctuation period in Fig. 13(b), though the range of the primary fluctuation period is larger with messier periodicity, compared with the Morlet wavelets (Fig. 13 (c)). Due to the outstanding smoothness and continuity, the Morlet wavelets outperform the other two types of wavelets transform techniques in capturing the signal's periodicity, as both amplitude and phase information can be revealed via coefficients modulus. Additionally, the performance of results based on the three wavelet basis functions for processing neutral current in terms of signal-to-noise ratio (SNR) have been compared, as both mean squared error (MSE) and computational efficiency are presented in Table 6. The results demonstrate that the Morlet wavelet achieves superior performance with minimal SNR and MSE for neutral current analysis, given the low sampling frequency (1 Hz) of neutral current signals. The computational duration is roughly less than 1 s, thus here the computational efficiency is not considered temporarily. Considering the characteristics of these three wavelet basic functions with the corresponding transform results from 5 substations, the Morlet wavelet is ultimately selected as the basic function for accomplishing the wavelet transform of neutral current.

4. The period analysis based on wavelet transform

Due to the differences existing in operational time, traction conditions and surrounding soil resistivity for different metro lines, the leakage current generated from different metro lines within the city varies transiently, as it is challenging to trace the source of leakage origins. If based on the periodicity of metro lines, the correlation between the leakage current from metro and the neutral current measured at substations can be figured out to some extent. Thus, the features involved in the neutral currents measured at substations need to be explored via certain advanced techniques, for evaluating the currents invading the neutral point of substations contributed by different metro lines.

The frequency domain analysis process with the application of the wavelet transform methodology is presented in the Fig. 14, the specific steps are demonstrated as: 1) Via applying the wavelet transform of the measured neutral current data, the primary fluctuating periods can be identified based on the variance of wavelet coefficients or the map of coefficients modulus; 2) Additionally, the wavelet coherence plot can be

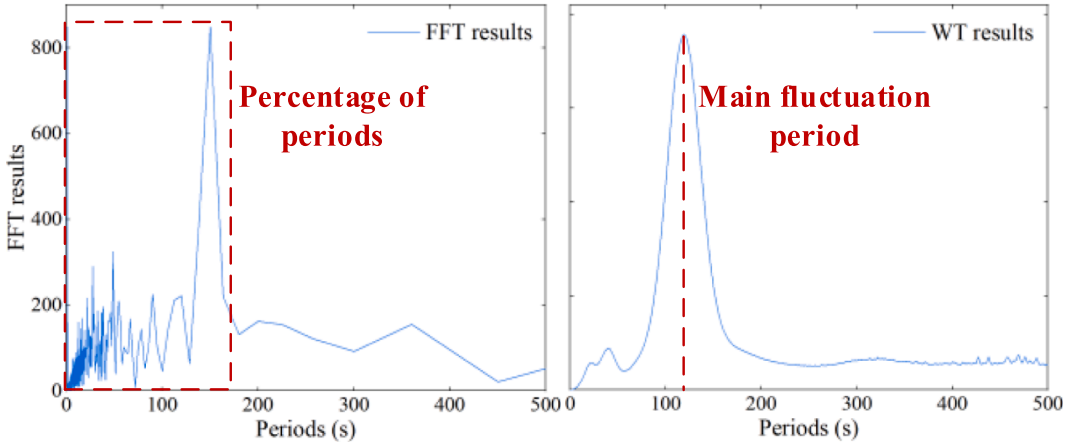

Fig. 12. The period analysis results via FFT and wavelet transform.

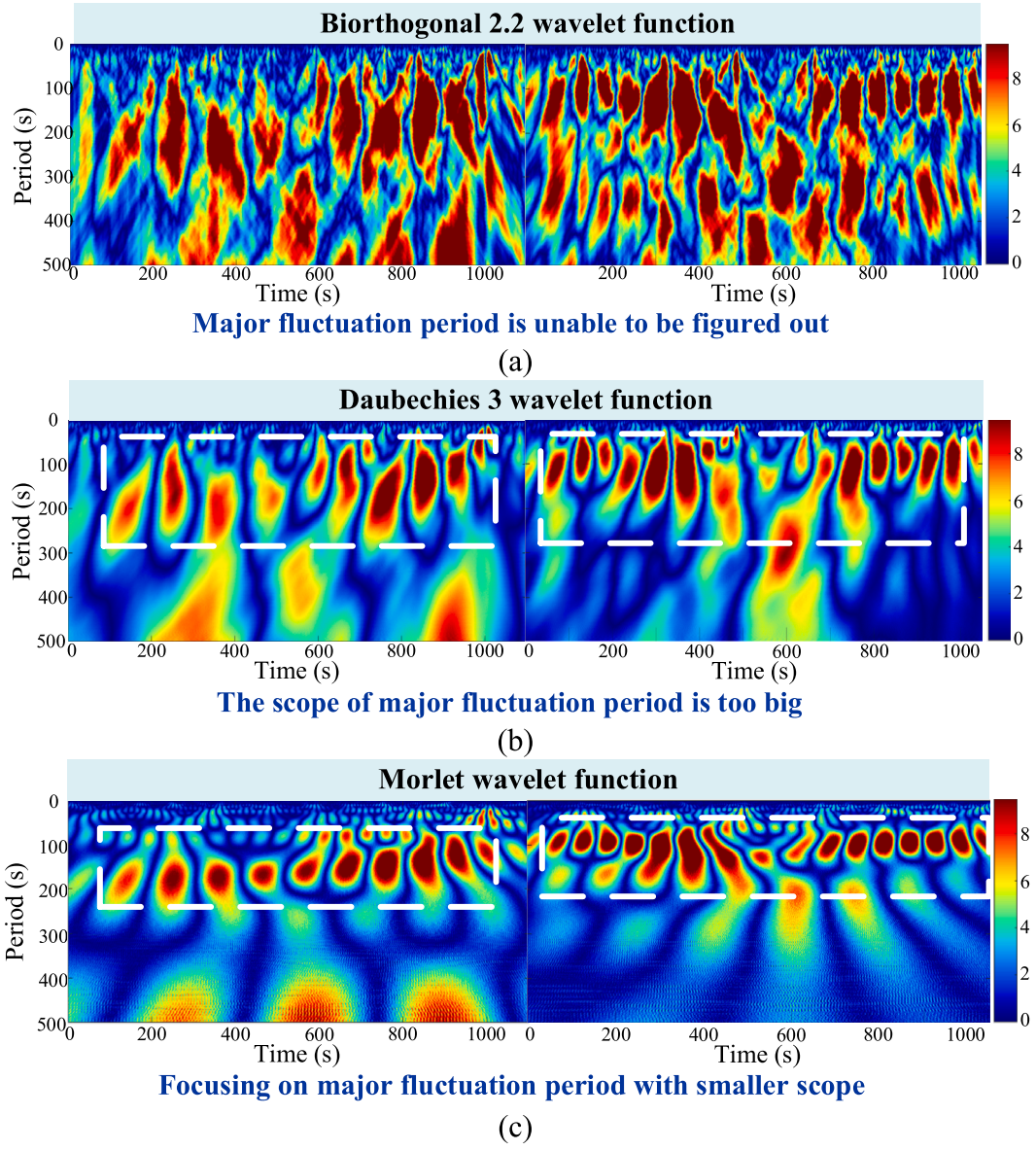

Fig. 13. The comparison of wavelet transform results applying 3 different basis functions: (a) Biorthogonal Wavelets; (b) Daubechies Wavelets; (c) Morlet Wavelets.

Table 6
The Comparison of Three Mother Wavelets.

Index	Morlet Wavelets	Daubechies Wavelets	Biorthogonal Wavelets
Signal to Noise Ratio (SNR)	32.5 dB	21.1 dB	26.8 dB
Mean Squared Error (MSE)	0.015	0.028	0.022
Computing efficiency (Second/Sample)	0.45	0.28	0.31
Applicable objects	The frequency analysis of non-stationary signal	Sparse signal	Signal denoising

used to validate the correlation between the traction current of metro and the neutral current of substations; 3) Through comparing the modulus of the wavelet coefficients between the stray current measured at the origin and the neutral current measured at the substation, the local periodic contributions of different metro lines can be clarified, for laying the solid foundation of the precise suppression on stray current source.

4.1. The selection of the substations and metro lines for correlation exploration

The selected region with 6 metro lines and 5 substations is shown in Fig. 15. The shortest distances between each substation and its adjacent metro lines are listed in Table 7. Substation 1 is similar to Substation 2, with two metro lines located nearby, while Substation 3 only has one metro line nearby. In contrast, the distances between the two metro lines near Substations 4 and Substation 5 differ significantly, which indicates that there might be a huge difference in the contributions brought from the two metro lines on the neutral currents at these substations due to the difference in physical distances.

Substation 1 is similar to Substation 2, with two metro lines located nearby, while Substation 3 only has one metro line nearby. In contrast, the distances between the two metro lines near Substations 4 and Substation 5 differ significantly, which indicates that there might be a huge difference in the contributions brought from the two metro lines on the neutral currents at these substations due to the difference in physical

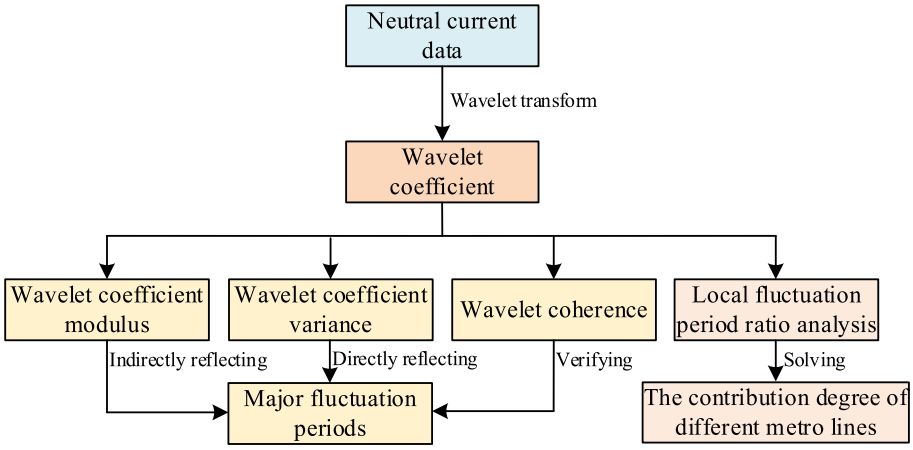

Fig. 14. The frequency-domain analysis based on the Wavelet Transform method.

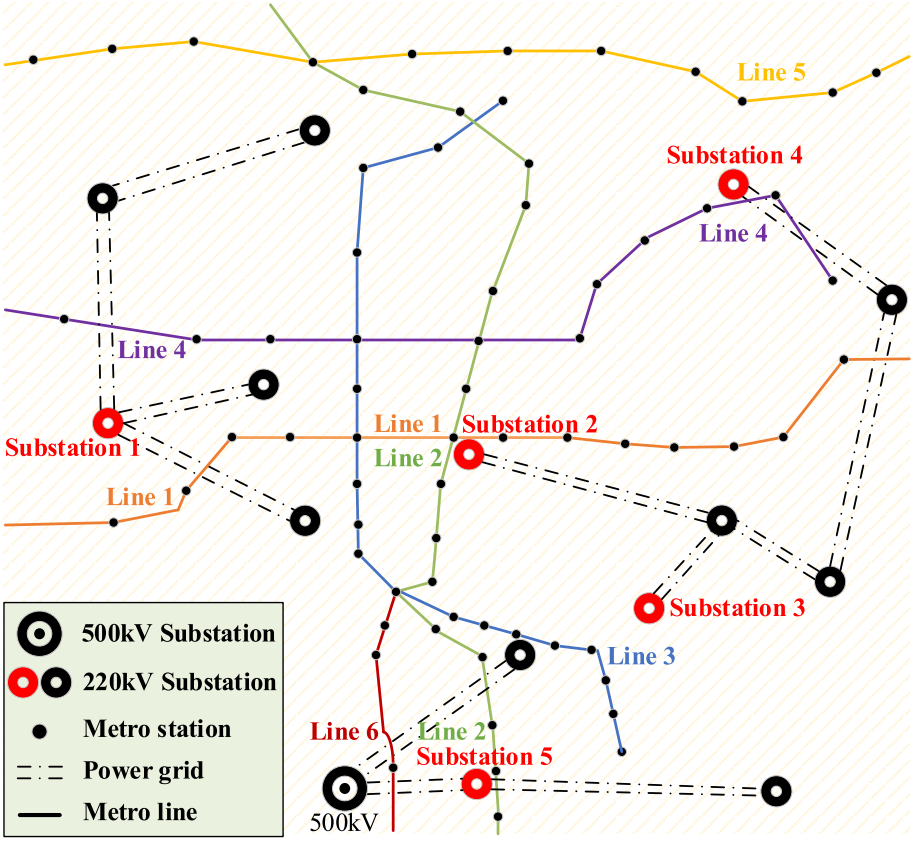

Fig. 15. The distribution of metro lines, metro stations, and substations.

Table 7
The Direct Distances between Each Substation and Metro Lines.

Substation No.	Neighboring metro lines	Distance/ m	Neighboring metro lines	Distance/ m
1	Line 1	1423	Line 4	1452
2	Line 1	140	Line 2	379
3	Line 3	1525	/	/
4	Line 4	202	Line 5	1340
5	Line 2	206	Line 6	2320

distances.

4.2. The correlation between wavelet-based frequency analysis results and metro operation cycles

The fluctuating characteristics of the neutral current of the substation may directly correspond to the operation intervals of surrounding metro lines. To verify the validity of this hypothesis, the wavelet waveform technique as an effective is applied to explore the feature of the neutral current of several substations, as the operational durations of each of metro lines between adjacent stations are shown in Fig. 16.

Initially, Substation 1 taken as an example here, is mainly impacted by the surrounding metro lines—Metro Line 1 and Metro Line 4, as

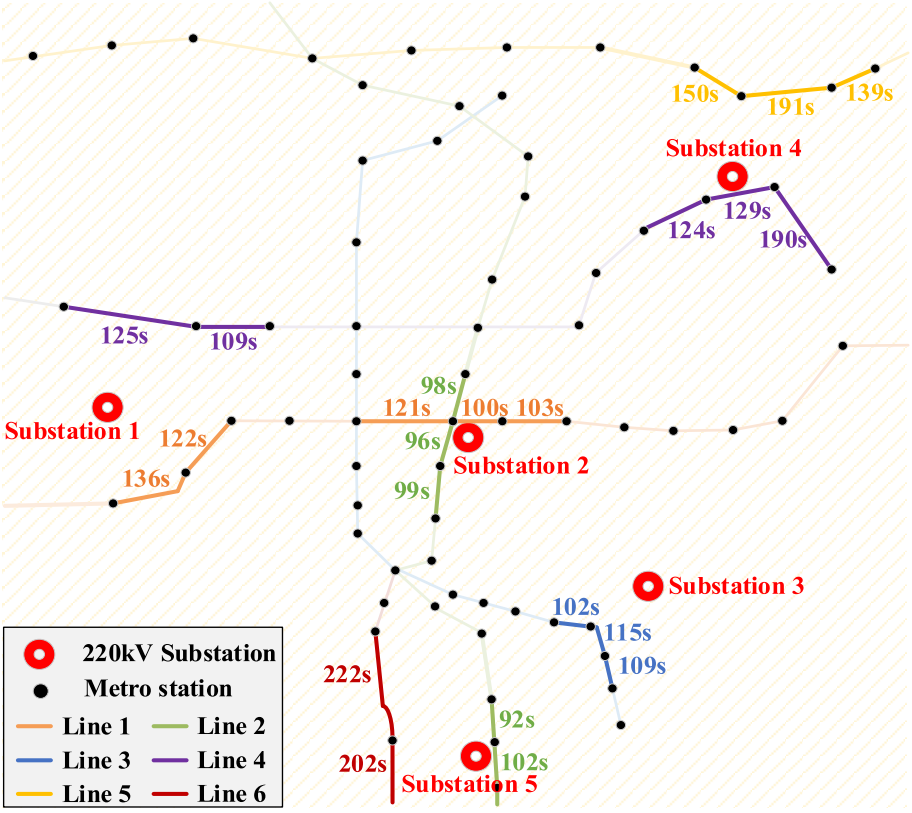

Fig. 16. The travel duration within the section between adjacent stations of neighboring metro lines.

presented in Table 3. In Fig. 17, the wavelet coefficient modulus is presented during the operational peak and non-operational periods of these two metro lines, as the wavelet coefficient modulus of the neutral current reaches its maximum at about 120 s, indicating that the primary fluctuation period is around 120 s. By contrast, during non-operational hours of metro lines, the waveform of wavelet coefficients lacks distinct periodic characteristics.

The coherence between the neutral current of Substation 1 and the traction current of two Metro Lines is shown in Fig. 18. It indicates the strong correlation existing between stray current and neutral current in the fluctuation period around 128 s, with the phase of the transformer neutral current slightly lagging behind the metro traction current.

The wavelet coefficient variances are calculated for the neutral currents achieved from different substations to verify the validity of the wavelet transform analysis method. As shown in Fig. 19(a), The travel duration within the section between adjacent stations of the two metro lines near Substation 2 is 96 s and 100 s respectively, closely matching the primary fluctuation period of the Substation 2's neutral current. In Fig. 19(b), the neutral current of Substation 3, which is located near a single metro line with an operation cycle of 115 s, shows a primary fluctuation period of 107 s, again consistent with the operational condition of Metro Line 3.

In contrast, two metro lines near Substation 4 and Substation 5 have significant differences in periodic duration between adjacent stations, resulting in the neutral current showing two ripple crests, corresponding to the operation of the metro lines (Fig. 20). Based on the scenarios of these five Substations, it can be found that the varying tendency of the substation's neutral current closely align with the operational periodicity of the surrounding metro lines.

The average error in fluctuation period analysis across the five substations is approximately 4.8 % (95 % CI: ±3.5 %). Based on the scenarios of these five Substations, it can be found that the travel time is

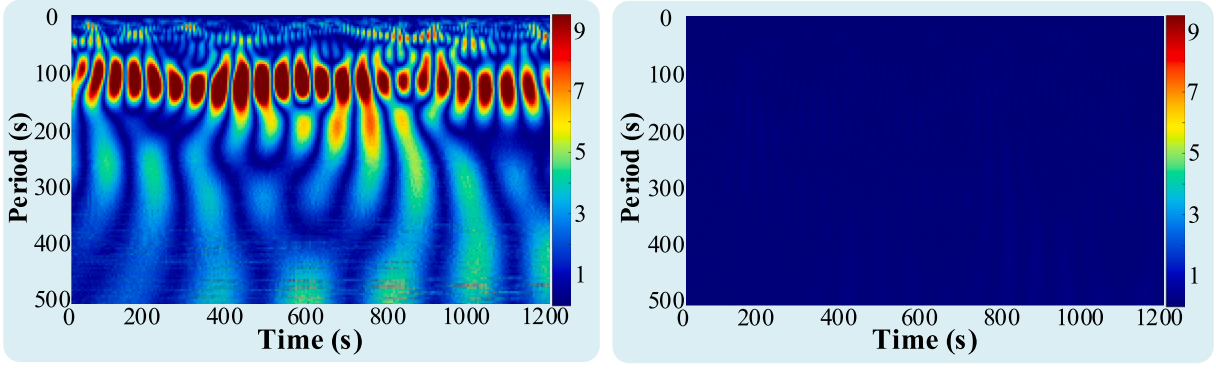

(a) On operation (b) Out of service

Fig. 17. The wavelet coefficients modulus of neutral current from Substation 1 at different time.

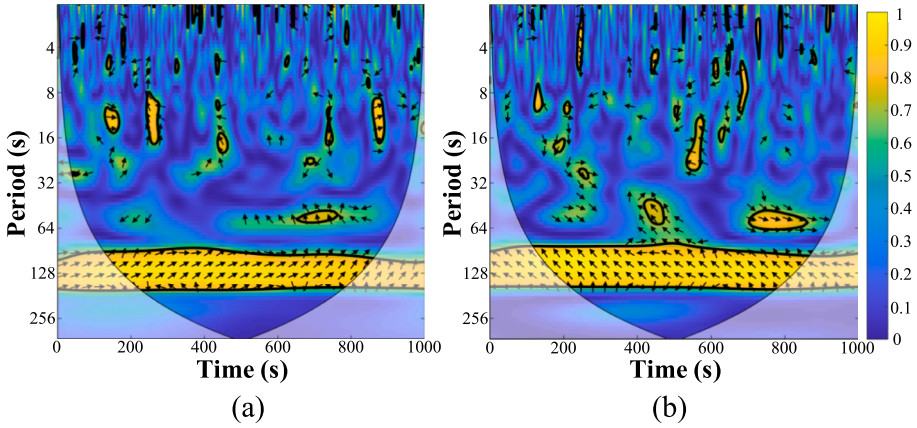

Fig. 18. The coherence of substation 1 neutral current with metro traction current.

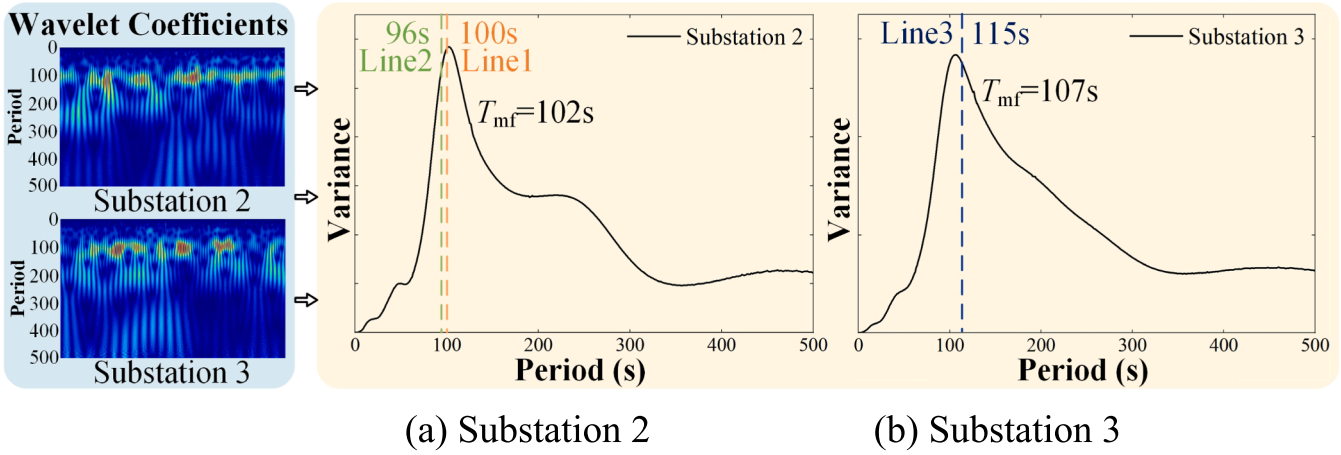

Fig. 19. The wavelet variance of neutral current from Substation 2 and Substation 3.

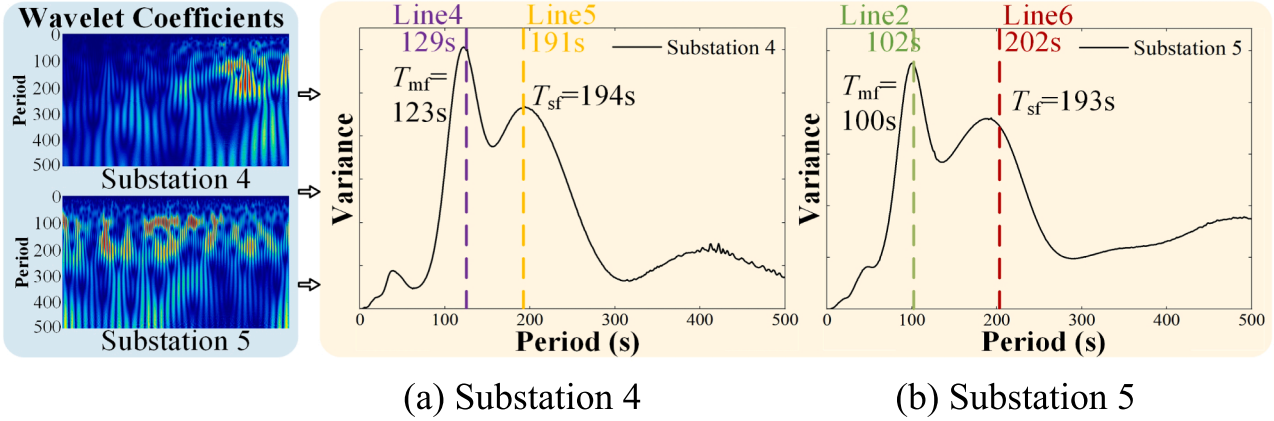

Fig. 20. The wavelet variance of neutral current from Substation 4 and Substation 5.

basically consistent with the neutral current fluctuation period.

To verify the consistency of the periodicity analysis of both neutral and traction currents between simulating and experimental results, Substation 2 during the peak hours is selected as an example here, as the operational duration of the surrounding metro lines (Metro Line 1 and Metro Line 2) between the adjacent stations is initialized as the same as the actual scenario, respectively, with trains departing every 4 min. The same wavelet analysis method is applied to address the simulating neutral current data, as the wavelet coefficient modulus with variance achieved from both simulation and experiments are presented in Fig. 21 (a) and Fig. 21(b) respectively. The primary fluctuation period obtained from simulated results closely aligns with the pre-set operational periodicity of the metro running between adjacent stations, further validating the correlation between the fluctuation period of neutral current and the operational duration of the metro line. The deviation between the period extracted from the neutral current of Substation 2 and the traction current from different metro lines is maintained at approximately below 4.9 %, as it can be viewed that the travel time is basically

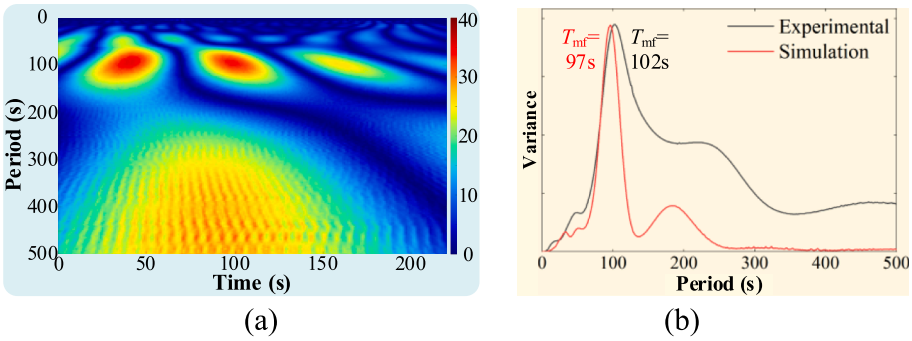

Fig. 21. The coefficient modulus and variance of simulated neutral current from substation: (a) The coefficient modulus; (b) The variance.

consistent with the neutral current fluctuation period.

4.2.1. Stray current contribution degree analysis based on transformer neutral current fluctuation period

Since the wavelet transform results via the Morlet wavelet basic function perform ideal accuracy at the local region, it is possible to obtain the wavelet coefficient modulus of the neutral current across various periods within a specific time range.

The wavelet coefficient modulus ratio of Substation 2 neutral current is shown in Fig. 22 over 30 min during non-operational hours, peak hours, and normal operation hours respectively. It can be found that the ratio of fluctuation periods corresponding to the operational duration of the metro between adjacent stations performs the largest during the peak hours, which indicates more often operation of surrounding metro lines directly resulting in a larger proportion of fluctuation periods in the neutral current of Substation 2.

Noteworthily, the two metro lines near Substation 1 have almost synchronous periodicities, whereas the two surrounding metro lines of Substation 2 have a difference of nearly 20 min in their operational duration as shown in Fig. 23. During Interval 1, both the Metro Line 1 and Metro Line 2 is under the operational condition, while only the Metro Line 2 is operating during the Interval 2. In the Interval 3, both of the metro lines are out of service. To analyze the individual contribution degree of each metro line to neutral current, the 'fingerprint'—wavelet coefficients are extracted during these three typical intervals: both metro lines operating (Interval 1), only one metro line operating (Interval 2), and neither metro line operating (Interval 3).

The total wavelet coefficient modulus and the ratio of different periods for Substation 2 during these three periods are shown in Fig. 24. The wavelet coefficient modulus during Interval 3 (no metro line in service) mainly describes the interference factors brought from the environment which nothing to do with both Metro Line 1 and Metro Line 2. Through subtracting the wavelet coefficient modulus of Interval 3 from that of Interval 2, the relative contribution value of Metro Line 2 to the neutral current of Substation 2 can be achieved. Similarly, subtracting the wavelet coefficient modulus of Interval 2 from that of Interval 1 yields the relative contribution value of Metro Line 1. During the fluctuation period between the 101th second and the 150th second,

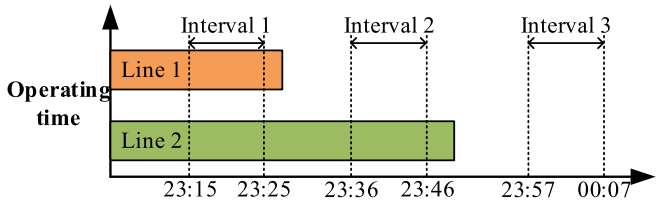

Fig. 23. The operational periodicities of the two metro lines near the Substation 2.

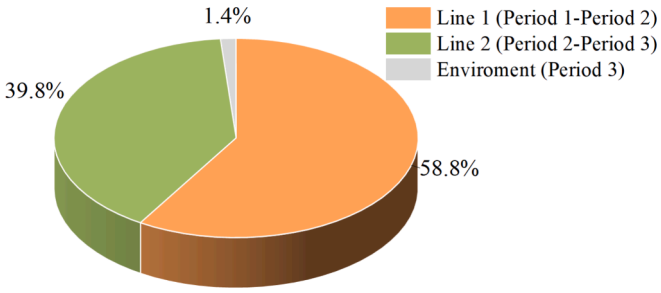

Fig. 24. The local fluctuation period ratio analysis of Substation 2 neutral current.

Metro Line 1 (located 100 m from Substation 2) contributes 58.8 % of the neutral current at Substation 2, while Metro Line 2 (300 m away) accounts for 39.8 %, which reveals that Metro Line 1's influence is 1.48 times greater than that of Metro Line 2 during this interval. The disparity highlights the critical role of spatial positioning in stray current distribution dynamics. Certainly, the physical distance between the metro line and the substation is only one element, as due to the difference in the time in service for these metro lines, the rail-ground insulating performance of Metro Line 1 is poorer than the case of Metro Line 2 as presented in Table 2.

To verify the consistency between the experimental and simulating results, Substation 2 is focused on here, as all the operational conditions

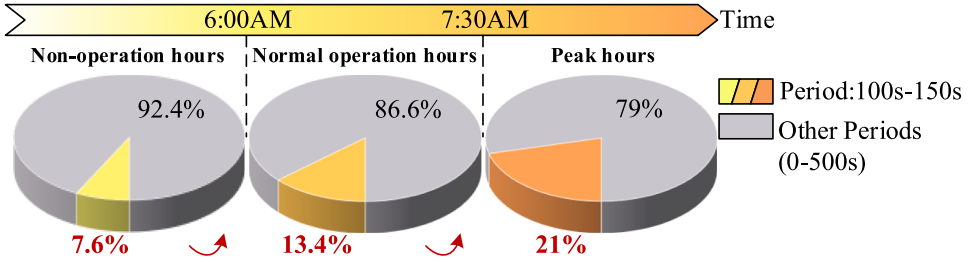

Fig. 22. Proportion of fluctuation periods in different time.

of the surrounding metro lines are initialized as same as in the practical case. The results of the wavelet analysis through the stray current model based on the BEM are presented in Fig. 25, as the contribution ratio of Metro Line 1 to Metro Line 2 is 59.3 % and 40.7 % respectively. The deviation of fluctuation periods in the neutral current of Substation 2 between the simulated and measured results is maintained within the 1.88 % average, which can be viewed as acceptable.

Via a series of the simulating and experimental tests presented above, the feasibility of the fluctuation period contribution analysis method is validated, as even when the substation is surrounded by multiple metro lines with different operational periodicity, the individual contributions from different substations to the neutral current of the substation can still be distinguished through the differences existing in their operating periodicity.

5. Conclusion

So far, lack of effective method of tracing the origin of stray current under the scenario of complex metro networks, the mainstreamed suppression measure is installed the DC-bias suppressor at the neutral point of the substation, however, the suppressor with fixed impedance cannot cope with the transiently-varying stray current effectively. For analyzing the ingredient of the stray current invaded into the substation through the neutral point, an effective method of tracing the origin of stray current is proposed here, offering valuable insights for suppressing stray current. The main contributions are presented as follows:

1) Initially, a certain city with complex metro networks with multiple substations was selected as the research object. Based on the investigation of the geological condition, the soil resistivity, and the physical location of substations and metro lines in the focused region, a stray current analysis model is launched based on the boundary element method (BEM), as the deviation between simulating and measured results of the neutral currents in substations is maintained within 10 %, which verifies the precision of the simulating model to some extent. This simulation model provides a verification approach for the contribution degree analysis method.
2) The periodic variation pattern of the traction current measured from metro lines and the fluctuation characteristics of the neutral current captured at substations are extracted to explore the correlation between them. By comparing the performance of Fourier transform and wavelet transform with different basis functions in analyzing the fluctuation characteristics of the neutral current, it is concluded that the wavelet transform with the Morlet basis function is the most suitable method for extracting the neutral current's periodicity.
3) The wavelet coefficients and variance of neutral current at 5 substations were calculated. Meanwhile, the coherence coefficient between the neutral current and the traction current was also achieved, revealing that the coherence coefficient exceeded 0.95 in the relevant fluctuation periods. Additionally, there is only a 5 % difference existing between the primary fluctuation period of the neutral current and the operational duration between adjacent stations for surrounding metro lines. Based on a local fluctuation period ratio analysis method, the contribution of multiple metro lines to the neutral current at a substation can be evaluated in real-time with high precision. The simulation results closely match the measured results, with an average deviation maintained within 3.08 %, thus verifying the validity of this method.

CRediT authorship contribution statement

Ye Cao: Conceptualization, Data curation, Formal analysis, Methodology, Software, Validation, Visualization, Writing – original draft, Writing – review & editing. **Song Xiao:** Conceptualization, Funding acquisition, Investigation, Project administration, Resources, Writing – review & editing. **Jingdong Yan:** Conceptualization, Data curation, Formal analysis, Methodology. **Chenyang Liu:** Formal analysis, Software, Validation, Visualization, Writing – original draft. **Tiangeng Li:** Formal analysis, Investigation. **Xiao Liu:** Methodology. **Guangning Wu:** Conceptualization, Investigation, Software, Resources, Supervision, Writing – review & editing. **Yujun Guo:** Conceptualization, Funding acquisition, Investigation, Software, Resources. **Jiefu Hou:** Formal analysis, Software. **Yongdong He:** Software. **Xueqin Zhang:** Investigation, Project administration. **Nibishaka Erneste:** Data curation. **Jan K. Sykulski:** Investigation, Project administration.

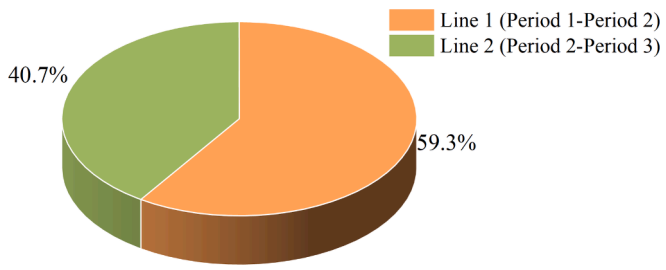

Fig. 25. The fluctuation periods in the neutral current of Substation 2 contributed by surrounding metro lines simulated via the stray current model based on BEM.

Declaration of competing interest

The authors declare that they have no known competing financial interests or personal relationships that could have appeared to influence the work reported in this paper.

Data availability

No data was used for the research described in the article.

References

[1] David R, Tad G. Determining the optimum installation of energy storage systems in railway electrical infrastructures by means of swarm and evolutionary optimization algorithms. Int J Electr Power Energy Syst 2021;124. https://doi.org/10.1016/j.ijepes.2020.106295.
[2] Ahmet D. Analyzing flexibility options for microgrid management from economical operational and environmental perspectives. Int J Electr Power Energy Syst 2024;158. https://doi.org/10.1016/j.ijepes.2024.109914.
[3] Zhang DL, Yang YL. Research on stray current monitoring of subway tracks. Mechatron Intell Mater I 2012;490–495(Pts 1-6):2494. https://doi.org/10.4028/www.scientific.net/AMR.490-495.2494.
[4] Bystrova OV. How we built the subway: about one story of the project 'History of factories and plants. Filologicheskie Nauki-Nauchnye Doklady Vysshei Shkoly-Philol Sci-Sci Essays High Educ 2022;5:171–8. https://doi.org/10.20339/PhS.5-22.171.
[5] Lin D, et al. Metro systems: construction, operation and impacts. Tunn Undergr Space Technol 2024;143. https://doi.org/10.1016/j.tust.2023.105373.
[6] Park J, Kang D. Evaluation of long-term durability of thermal insulation paint under aging conditions in railway sites. J Kor Soc Nondestruct Test 2022;42(1):43–50. https://doi.org/10.7779/JKSNT.2022.42.1.43.
[7] Fu WB, et al. A study on ignition criterion of a large carbon char particle. Combust Sci Technol 1995;108(1–3):91–101. https://doi.org/10.1080/00102209508960392.
[8] He Q, et al. Experimental analysis of transformer core vibration and noise under inter-harmonic excitation. Appl. Sci. 2022;12(3). https://doi.org/10.3390/app12031758.
[9] Liu CM, et al. Simulating the vibration increase of the transformer iron core due to the DC bias. Int J Appl Electromagn Mech 2017;55(3):423–33. https://doi.org/10.3233/JAE-160132.
[10] Do Nhu Y, et al. Effect of power quality on the performance of explosion-proof transformers in mining in Vietnam. Inz Miner - J Pol Miner Eng Soc 2023;2:65–9. https://doi.org/10.29227/IM-2023-02-13.
[11] Charalambous CA, Cotton I, Aylott P. Modeling for preliminary stray current design assessments: the effect of crosstrack regeneration supply. IEEE Trans Power Deliv 2013;28(3):1899–908. https://doi.org/10.1109/TPWRD.2013.2259849.
[12] Zhang J, Song X, Xiao L, Chen L, Wu G, Cui Y, et al. Simulation study of the influence of stray current on DC bias of power transformer. In: Proc 4th Int Conf Electr, Autom Mech Eng (EAME), Electron Network, Jun. 21–22. Vol. 1626; 2020. doi: 10.1088/1742-6596/1626/1/012061.

[13] Wang Y, Wen T, Yu F, Mao Y, Wu Q, Liu S, et al. A research on inductance forcedly absorbing current to reduce stray current in metro. In: Proc 2021 IEEE 16th Conf Ind Electron Appl (ICIEA), Chengdu, China, Aug. 1–4; 2021. p. 779–782. doi: 10.1109/ICIEA51954.2021.9516163.
[14] Fichera F, Mariscotti A, Ogunsola A. Evaluating stray current from DC electrified transit systems with lumped parameter and multi-layer soil models. In: Proc 2013 IEEE EUROCON, Zagreb, Croatia, Jul. 1–4; 2013. p. 1186–91. doi: 10.1109/EUROCON.2013.6625131.
[15] Song MK. Approximately coupled method of finite element method and boundary element method for two-dimensional elasto-static problem. J Korean Geosynthetic Soc 2021;20(3):11–20. https://doi.org/10.12814/ikgss.2021.20.3.011.
[16] Dong L, Yao ZL, Ge CG, Shi CJ, Chen JZ. Fourier analysis of the fluctuation characteristics of pipe-to-soil potential under metro stray current interference. Surf Technol 2021;50(2):294–303. https://doi.org/10.16490/j.cnki.issn.1001-3660.2021.02.031.
[17] Wang CT, Li W, Wang YQ, Yang XF, Xu SY. Development of a novel process of corrosion rate estimation of steel under stray current interference: Q235A pipe steel as an example. Russ J Electrochem 2021;57(5):448–61. https://doi.org/10.1134/S1023193521050141.
[18] Shen J, Zhao S, Chen J. Estimating harmful effect of dynamic stray currents on pipeline by simultaneous multi-parametric field measurements, continuous wavelet cross-correlation analysis, and frequency plots. Mater Corros-Werkstoffe Und Korrosion 2019;70(2):357–65. https://doi.org/10.1002/maco.201810310.
[19] Żakowski K, Darowicki K. Detection of stray current field interference on metal constructions using STFT. Key Eng Mater 2005;293–294:785. https://doi.org/10.4028/www.scientific.net/kem.293-294.785.
[20] Lin S, Tang Z, Chen X, Liu X, Liu Y. Analysis of stray current leakage in subway traction power supply system based on field-circuit coupling. Energies 2024;17(13). https://doi.org/10.3390/en17133121.
[21] Li C, Du Q, Guo Y, Liu Y, Yang F, Chen L, et al. Modeling of stray currents from metro intruding into power system considering the complex geological conditions in modern megacities. IEEE Trans Transp Electrific 2023;9(1):1653–63. https://doi.org/10.1109/TTE.2022.3179559.
[22] Nasir NAFM, et al. Impact of earthing system designs and soil characteristics on tower footing impedance and ground potential rise: a modelling approach for sustainable power operation. Sustainability 2021;13(15):8370. https://doi.org/10.3390/su13158370.
[23] Hou WB, Tan GJ, Li DL. Model predictive current control for the grid-connecting three-level NPC inverters based on an effective harmonic extraction method under a low-switching frequency. IEEJ Trans Electr Electron Eng 2022;17(8):1160–7. https://doi.org/10.1002/tee.23607.
[24] Hou WB, Ling Z, Li DL. Control design for the NPC three-level grid-connected converter with non-ideal grid system. Recent Adv Electr Electron Eng 2022;15(7):533–43. https://doi.org/10.2174/2352096515666220620100034.
[25] Madahi SSK, Abyaneh HA, Nucci CA, Parpaei M. A new DFT-based frequency estimation algorithm for protection devices under normal and fault conditions. Int J Electr Power Energy Syst 2022;142. https://doi.org/10.1016/j.ijepes.2022.108276.
[26] Mujezinovic A, Martinez S. Application of the continuous wavelet cross-correlation between pipe-to-soil potential and pipe-to-rail voltage influenced by dynamic stray current from DC train traction. IEEE Trans Power Del 2021;36(2):1015–23. https://doi.org/10.1109/TPWRD.2020.2999868.